

## Simulations of CVD Diamond Film Growth: 2D Models for the identities and concentrations of gas-phase species adsorbing on the surface

Paul W. May<sup>1</sup> and Yuri A. Mankelevich<sup>2</sup>

<sup>1</sup>School of Chemistry, University of Bristol, Bristol, BS8 1TS, United Kingdom.

<sup>2</sup>Skobel'tsyn Institute of Nuclear Physics, Moscow State University, Leninskie gory, Moscow 119991, Russia.

### ABSTRACT

A prerequisite for modelling the growth of diamond by CVD is knowledge of the identities and concentrations of the gas-phase species which impact upon the growing diamond surface. Two methods have been devised for the estimation of this information, and have been used to determine adsorption rates for  $C_xH_y$  hydrocarbons for process conditions that experimentally produce single-crystal diamond, microcrystalline diamond films, nanocrystalline diamond films and ultrananocrystalline diamond films. Both methods rely on adapting a previously developed model for the gas-phase chemistry occurring in a hot filament or microwave plasma reactor. Using these methods, the concentrations of most of the  $C_xH_y$  radical species, with the exception of  $CH_3$ , at the surface have been found to be several orders of magnitude smaller than previously believed. In most cases these low concentrations suggest that reactions such as direct insertion of  $C_1H_y$  ( $y = 0-2$ ) and/or  $C_2$  into surface C–H or C–C bonds can be neglected and that such species do not contribute significantly to the diamond growth process in the reactors under study.

### INTRODUCTION

Chemical vapor deposition (CVD) of diamond is a maturing technology that is beginning to find many commercial applications in electronics, cutting tools, medical coatings and optics [1]. The CVD process usually involves the gas-phase activation of a gas mixture containing a small quantity of a hydrocarbon in excess hydrogen [2]. A typical gas mixture uses a few %  $CH_4$  in  $H_2$  (plus sometimes additional Ar or  $N_2$ ), and depending upon the growth conditions this produces polycrystalline films with grain sizes from ~5 nm to mm. Films with grain sizes less than 10-20 nm are often called ultrananocrystalline diamond (UNCD) films; those with grain sizes a few 10s or 100s of nm are nanocrystalline diamond (NCD); those with grain sizes microns or tens of microns are termed microcrystalline diamond (MCD); and those with grain sizes approaching or exceeding 1 mm are single-crystal diamond (SCD).

In a hot filament (HF) or microwave (MW) plasma CVD reactor, the substrate is exposed to large number of hydrocarbon species, as well as to atomic H and C, and the interplay between various gas-surface processes, such as adsorption of hydrocarbon radicals (mainly  $CH_3$ ), etching, surface migration, and bonding to the diamond structure, controls the morphology and growth rate of the resulting diamond film. Using these ideas, and following a similar procedure to that of Netto and Frenklach [3], we developed a simplified one-dimensional kinetic Monte Carlo (KMC) model of the growth of diamond films [4], initially for a fixed set of process conditions and substrate temperature. Although the model was only 1D, the interplay between adsorption,

etching/desorption and addition to the lattice was qualitatively modelled using known or estimated values for the rates of each process. More recently we extended the KMC model of SCD growth to include the temperature dependence of the various surface processes [5]. Our most recent KMC paper [6] involves simulating diamond growth using as input data the experimental reactor conditions used to deposit SCD, MCD, NCD and UNCD. The first consideration was that for some conditions (e.g. those used for UNCD deposition) the concentrations of other  $C_1$  species, in particular C atoms, may no longer be negligible in comparison to that of  $CH_3$ . Thus, we needed to determine the rates of adsorption for *all* relevant hydrocarbon radical species onto the surface, and decide their subsequent fates. Some of this information can be determined spectroscopically [7], however, we now describe how the data from previously published [8] simulations of the gas-phase chemistry can be re-evaluated in order to estimate the concentrations for all the important  $C_1$  species at the diamond surface.

## THEORY

In order to study a range of deposition conditions used for growth of different types of diamond we require knowledge of the concentrations of atomic H,  $CH_3$  and the remainder of the other  $C_1$  hydrocarbon radicals (C, CH,  $CH_2$ ) at the growing diamond surface, all as a function of deposition conditions (pressure,  $T_s$ , *etc.*). These parameters have been calculated using the finite-difference model described in Ref.[8] for the gas mixtures and conditions used experimentally to deposit SCD, MCD, NCD and UNCD in both hot filament (HF) and microwave (MW) reactors. Briefly, MCD conditions are 1%  $CH_4/H_2$  at 20 Torr in a HFCVD reactor with substrate temperature  $T_s \sim 1173$  K; NCD conditions are the same except using 5%  $CH_4/H_2$ ; UNCD(HF) conditions used the same reactor but with 80% Ar/18.5%  $H_2/1.5\%CH_4$  at 100 Torr; UNCD(MW) films were deposited using 1%  $CH_4/1\%H_2/98\%Ar$  in a 700 W MW plasma at 170 W and a reduced  $T_s \sim 873$  K; and SCD conditions are for a high density, 600 W MW plasma at 180 Torr using 10%  $CH_4/H_2$  and  $T_s \sim 973$  K.

The model uses a database of known chemical reactions along with their temperature-dependent rates to calculate a steady-state gas composition throughout the plasma ball or filament-to-substrate region. The model calculates the concentrations of species as a function of position,  $z$ , above the diamond surface, but is restricted in resolution to the grid size,  $dz$ , the value of which was chosen to be 0.5 mm based upon the limitations of computation speed. Figures 1(a) and 1(b) show an example of such data for SCD conditions for a sub-set of the species present. The data in Fig.1 taken from Ref. [8] for species concentrations *near* the substrate equate to a distance of  $z = 0.5$  mm in the model. Previously we have assumed that the species concentrations at the surface ( $z = 0$ ) can be taken to be the same as those calculated at  $z = 0.5$  mm. However, near the surface there is often a thin boundary layer ( $<1$  mm) in which temperatures, gas flows and concentrations can change significantly. Previously, the only species considered to have any significant effect upon diamond growth were H and  $CH_3$ , which (as can be seen in Fig.1(b)) have relatively weak dependences of concentration with  $z$  for  $z < 5$  mm, despite the steep temperature drop over this distance. As a result, our previous assumption that the concentration of  $CH_3$  at  $z = 0$  can be taken to be the same as that at  $z = 0.5$  mm is reasonable. However, such an assumption would be incorrect for the other hydrocarbon species, whose dependences of concentration with  $z$  near the surface are much stronger. We have tackled this problem using two approaches:

## **Method A**

In the first approach, we found that power-law expressions of the form  $[X] = pz^q$ , where  $[X]$  is the concentration of a given species at position  $z$ , and  $p$  and  $q$  are constant fitting parameters, fitted the concentration dependences of all the species between  $z = 5$  mm to  $z = 0.5$  mm reasonably accurately (see Fig. 1(b)). Extrapolation of these expressions to smaller  $z$  allows  $[X]$  for each species to be estimated at positions closer to the surface. However, extrapolation back to  $z = 0$  is clearly not acceptable, as this would always give  $[X]_s = 0$  (where the subscript 's' denotes at the surface), and also would be incorrect on physical grounds as the position and effect of any boundary layer are unknown. Therefore, a degree of subjective judgment is required as to the  $z$ -position at which the extrapolation becomes invalid. For most species this will be a moot point, as once  $[X]_s$  falls below  $\sim 10^9$  cm<sup>-3</sup> that species will have negligible influence on the growth chemistry. Nevertheless, a position needs to be chosen, and we have used 0.05 mm as the threshold, as this is roughly equivalent to the mean free path of molecules at process pressures 100-200 Torr. In other words, we take  $[X]_s \sim [X](z = 0.05$  mm), and assume that the cases where this may be inaccurate (maybe even by a couple of orders of magnitude) are irrelevant since at that position  $[X] < 10^9$  cm<sup>-3</sup>. The extrapolated concentrations for many of the important species for 4 diamond deposition conditions are given in Table I.

## **Method B**

The second approach to estimating  $[X]_s$  from the data in Fig.1 is to treat the gas close to the surface as being simply a compressed version of the gas at the top of the plasma ball (or above the filament). In doing so, we ignore the effect of any temperature jump  $\Delta T$  near the substrate surface, because, for all conditions under study, calculations based on the literature data<sup>9</sup> for similar systems show that  $\Delta T < 60$  K and is, therefore, negligible. With this approximation we can take the chemistry occurring at the top of the plasma ball to be an analogue for that near the surface. The disadvantage of this approach is that it neglects any differences in diffusional transfer terms. The advantage is that an arbitrary extrapolation threshold is no longer needed; we simply find the  $z$ -position in the plasma at which the gas temperature is the same as the surface temperature ( $T_g(z) = T_s$ ) and take the concentrations of all the species at this  $z$ -position,  $[X](z)$ , to be an estimate for  $[X]_s$ . These values are also shown in Table I, and in most cases are similar to those obtained using the first approach.

Note that the atomic hydrogen concentration at  $z = 0$ ,  $[H]_s$ , is a special case as a result of the substantial loss of H atoms at the substrate and substrate-holder surfaces due to H-abstraction and addition reactions. Thus,  $[H]_s$  was calculated using a more elaborate diffusion model taking account of losses and reactions at the surface [8], and is also given in Table I.

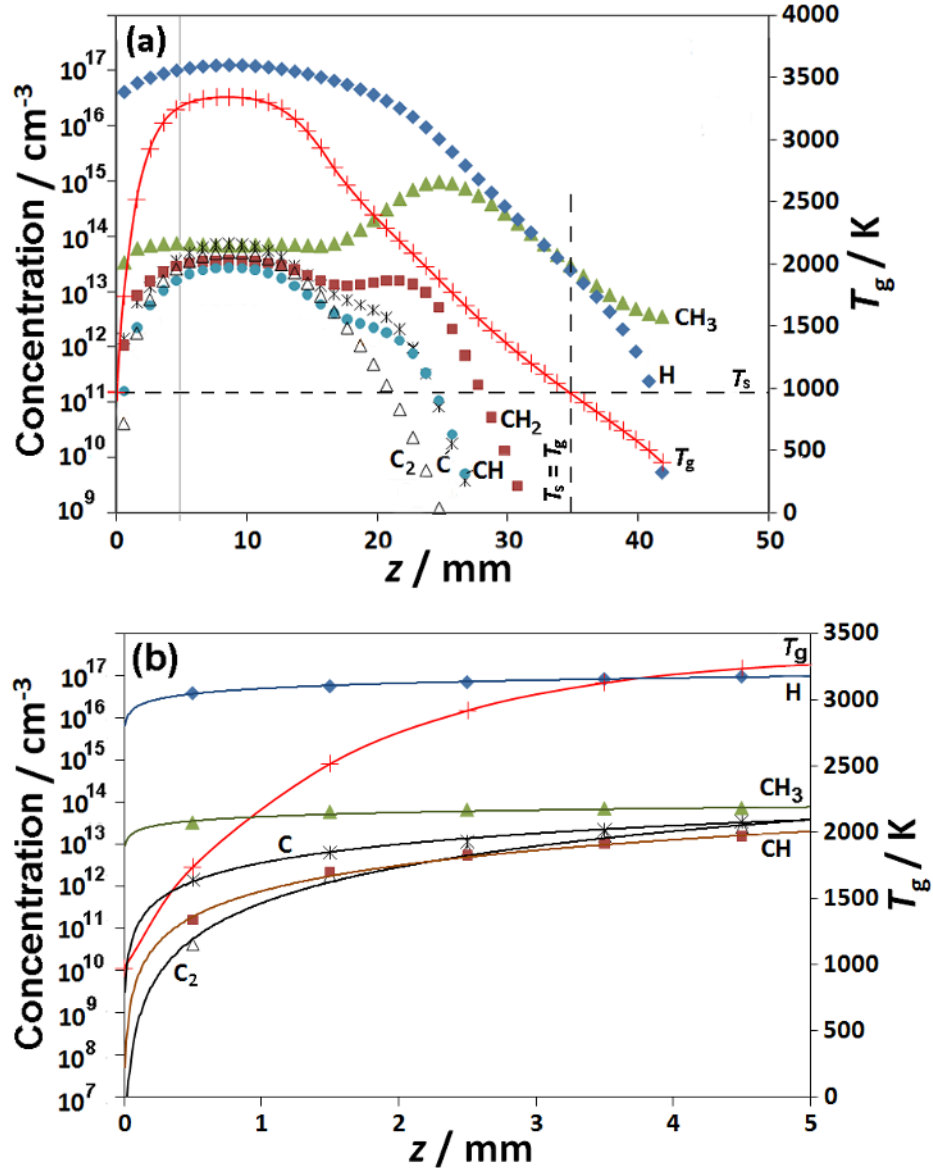


**Figure 1.** Concentrations of a sub-set of the gas-phase species above a diamond surface for MW plasma SCD conditions calculated using the model described in Ref.[8]. (a) The full data set from  $z = 0$  to  $z = 50$  mm, with a dashed vertical line showing the position ( $z = 34.5$  mm) where in this case the gas temperature equals the substrate temperature ( $T_g = T_s$ ) used in Method B. (b) The same data on an expanded scale near the substrate. The best-fit lines using power-law expressions used in Method A are also shown with their extrapolations back to near  $z = 0$ .

## RESULTS

The full concentration profile for SCD, MCD, NCD and UNCD conditions are shown in Figs.1-4. Using either Method A or B for all 4 deposition conditions we find that the concentration of  $\text{CH}_3$  at the surface only decreases by a factor of 2 or 3 from that at  $z = 0.5$  mm, which means that previously published results [4,8] which used the higher value for  $[\text{CH}_3]$  are not significantly affected and are still valid.

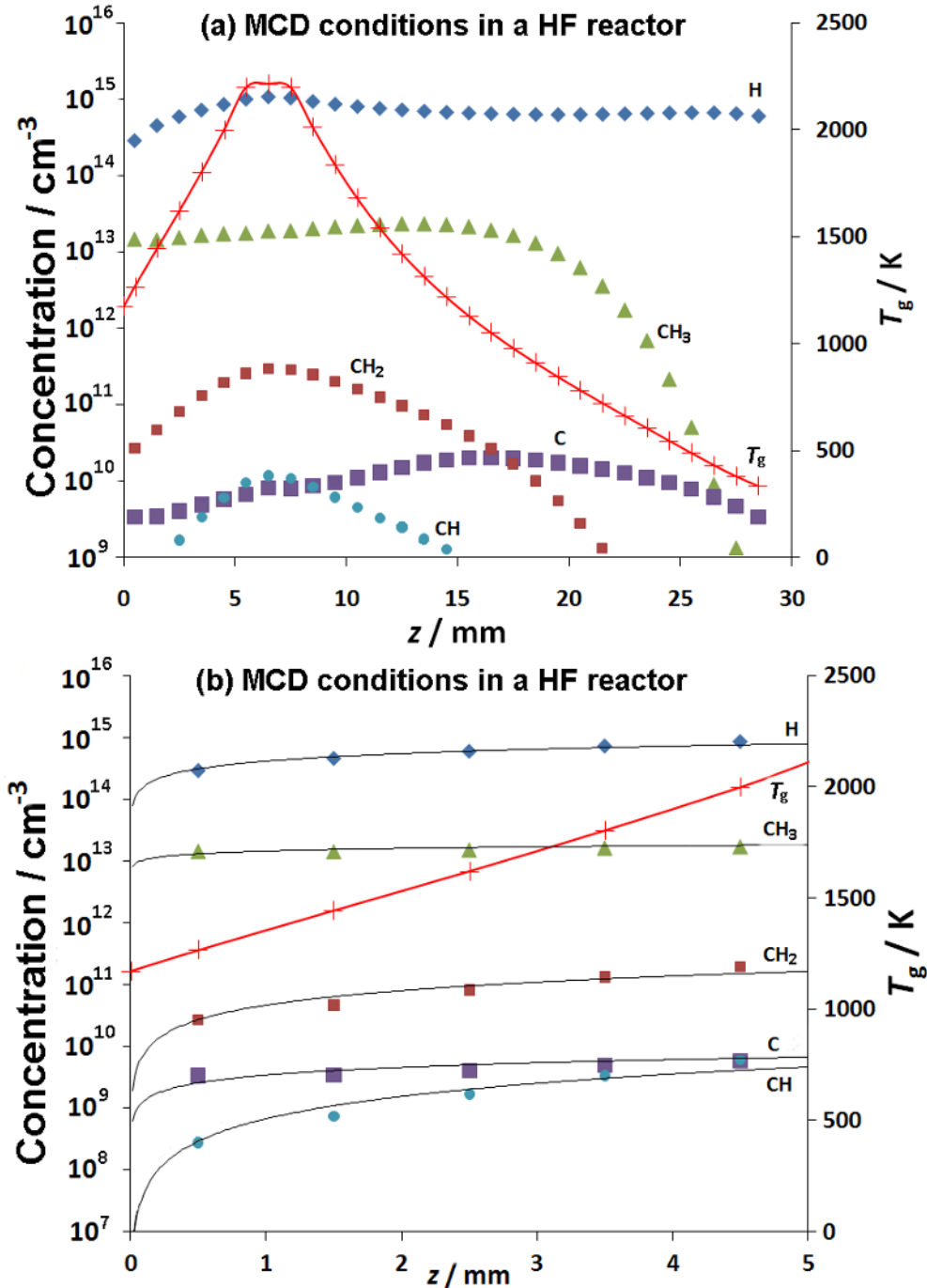


**Figure 2.** Concentrations of a sub-set of the gas-phase species above a diamond surface for HF MCD growth conditions calculated using the model in Ref.[8]. (a) The full data set from  $z = 0$  to  $z = 50$  mm. (b) The same data on an expanded scale near the substrate. The best-fit lines using power-law expressions used in Method A are shown with their extrapolations back to near  $z = 0$ .

The main finding is that the new estimated surface concentrations for many of the more reactive species, including C, CH, and CH<sub>2</sub>, are all smaller by a few orders of magnitude than their values at  $z = 0.5$  mm. A word of caution, however. These estimates, and even those based on the best equilibrium approach, *e.g.* finite-difference calculations with a very fine grid

( $dz \ll 0.5$  mm), do not take into account the unknown position and sharp temperature gradients associated with the non-equilibrium boundary-layer. In MW CVD reactors, especially, these temperature gradients may be very sharp, so in these cases both Methods A and B may underestimate the real fluxes of some reactive species on the substrate.

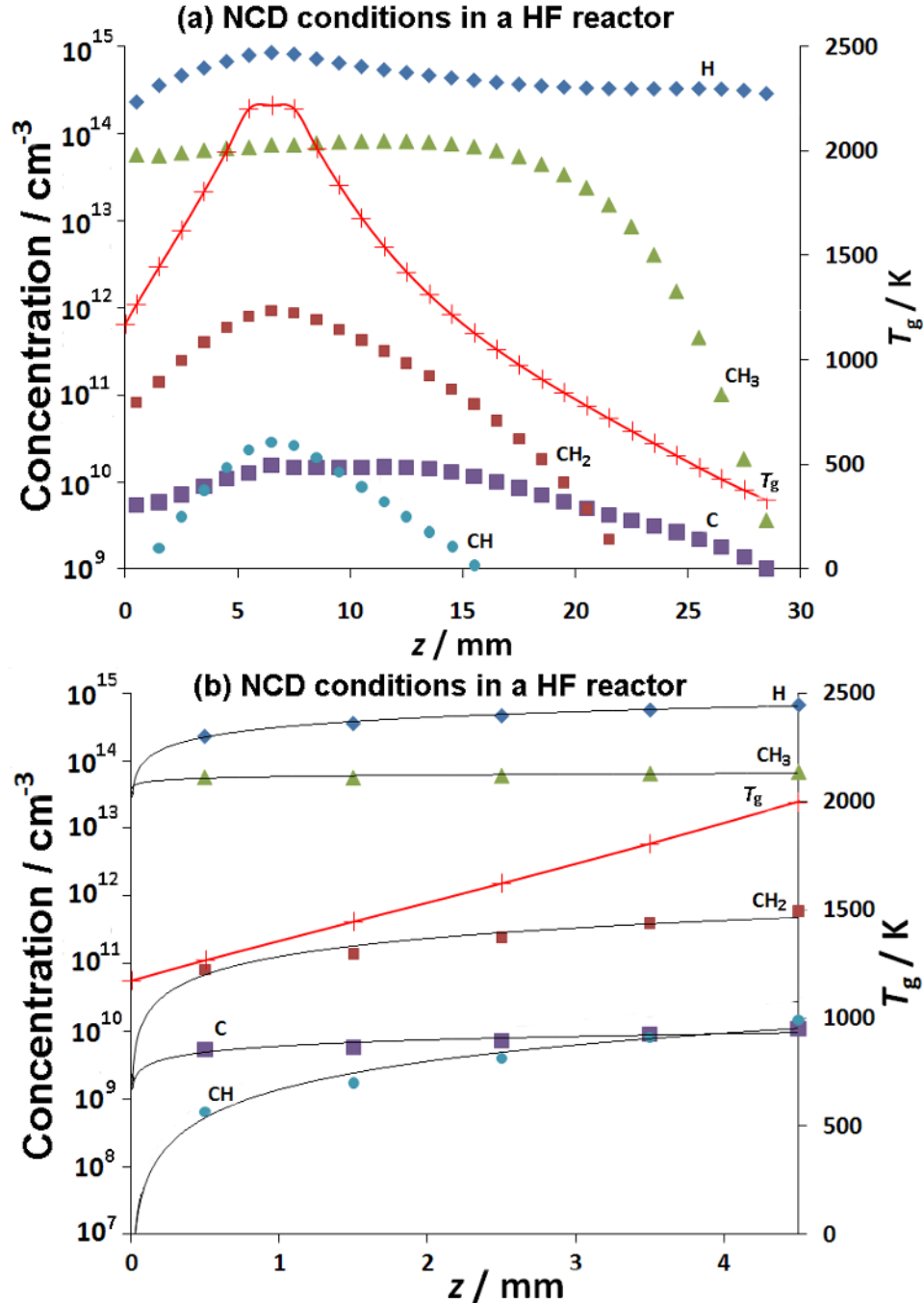


**Figure 3.** As for Fig.2(a) and (b), but for HF NCD growth conditions.

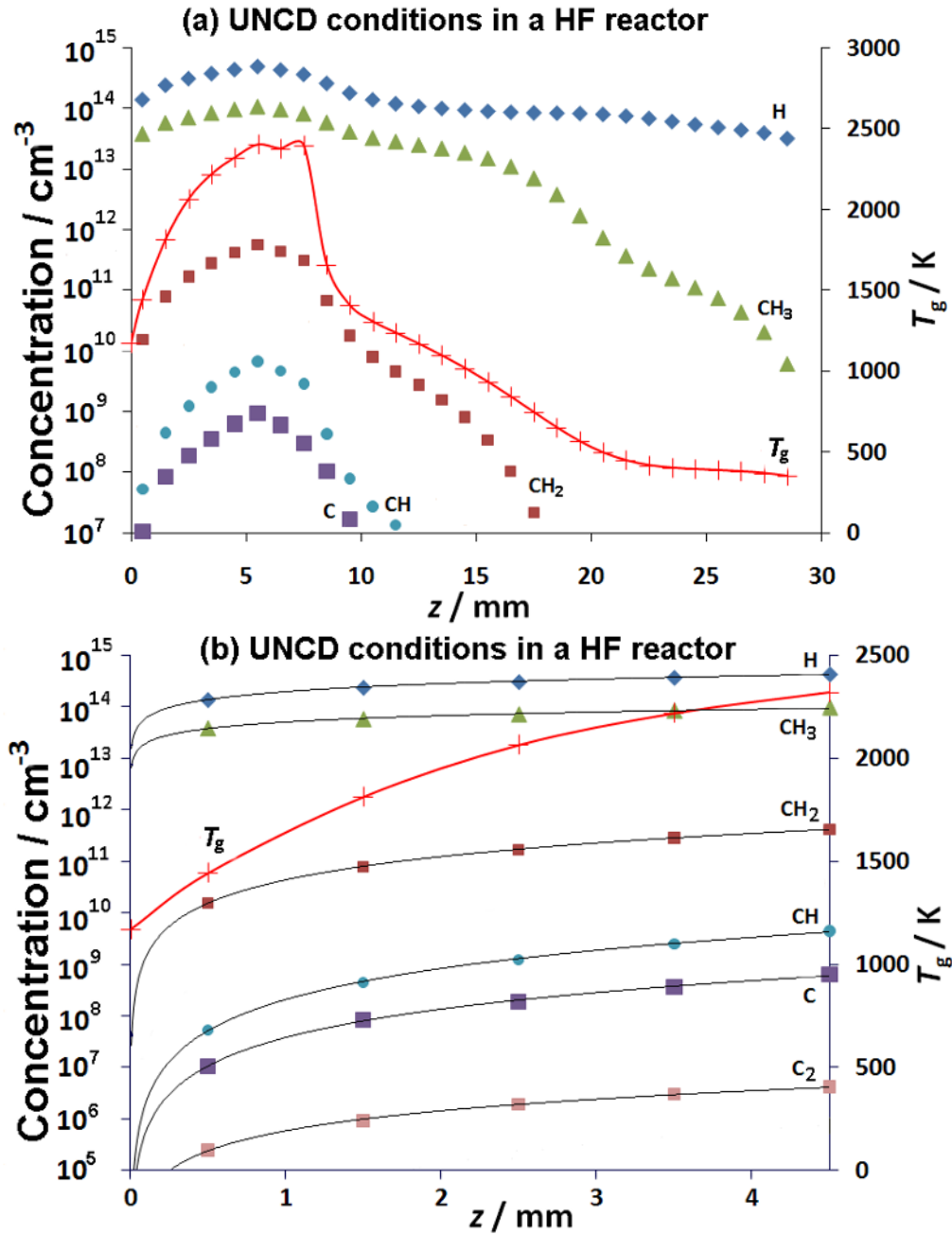


**Figure 4.** As for Fig.2(a) and (b), but for HF UNCD growth conditions.

## CONCLUSIONS

The fact that the new estimated surface concentrations for many of the more reactive hydrocarbon radicals are smaller by a few orders of magnitude than their values at  $z = 0.5$  mm has important implications for diamond growth. These very low concentrations effectively rule out C, CH,  $\text{CH}_2$ ,  $\text{C}_2$  and most other  $\text{C}_x\text{H}_y$  hydrocarbon radical species as being significant factors in the diamond growth mechanism for all types of diamond, leaving  $\text{CH}_3$  as the dominant growth species. These lower estimates for surface concentrations will also be important information for

workers studying the effect of these species upon defect formation or  $sp^2$  C content in diamond films (e.g. Refs.[10,11]), and the relative importance of these species may need to be re-evaluated.

**TABLE I.** Concentrations,  $[X]_s$ , (in  $\text{cm}^{-3}$ ) of selected gas-phase species at the surface for different experimental diamond film growth conditions [8].  $[X]_s$  values have been estimated using Methods A and B described in the text.  $\text{CH}_2(\text{s})$  refers to the singlet state, while  $\text{C}_2(\text{X})$  and  $\text{C}_2(\text{a})$  are the ground-state and first excited-state of  $\text{C}_2$ , respectively.

X	SCD		MCD		NCD		UNCD	
	A	B	A	B	A	B	A	B
H	$3.4 \times 10^{16}$	$3.4 \times 10^{16}$	$1.9 \times 10^{14}$	$1.9 \times 10^{14}$	$1.5 \times 10^{14}$	$1.5 \times 10^{14}$	$3.0 \times 10^{13}$	$3.0 \times 10^{13}$
$\text{CH}_3$	$1.0 \times 10^{13}$	$2.9 \times 10^{13}$	$8.0 \times 10^{12}$	$2.2 \times 10^{13}$	$6.0 \times 10^{13}$	$7.3 \times 10^{13}$	$8.0 \times 10^{12}$	$2.5 \times 10^{13}$
$\text{CH}_2$	$1.0 \times 10^{10}$	$5.7 \times 10^6$	$1.0 \times 10^9$	$4.5 \times 10^{10}$	$2.0 \times 10^9$	$1.0 \times 10^{11}$	$1.0 \times 10^8$	$2.8 \times 10^9$
$\text{CH}_2(\text{s})$	$1.0 \times 10^8$	$6.4 \times 10^5$	$1.0 \times 10^6$	$6.9 \times 10^8$	$5.0 \times 10^6$	$1.0 \times 10^9$	$1.0 \times 10^5$	$7.0 \times 10^7$
CH	$5.0 \times 10^8$	$2.4 \times 10^3$	$1.0 \times 10^6$	$1.1 \times 10^9$	$1.0 \times 10^6$	$1.4 \times 10^9$	$1.0 \times 10^4$	$7.6 \times 10^6$
C	$1.0 \times 10^{10}$	$1.3 \times 10^4$	$6.0 \times 10^8$	$1.9 \times 10^{10}$	$2.0 \times 10^9$	$1.2 \times 10^{10}$	$1.0 \times 10^4$	$9.3 \times 10^5$
$\text{H}_2$	$9.3 \times 10^{17}$	$9.3 \times 10^{17}$	$1.5 \times 10^{17}$	$1.5 \times 10^{17}$	$1.5 \times 10^{17}$	$1.5 \times 10^{17}$	$1.8 \times 10^{17}$	$1.8 \times 10^{17}$
$\text{C}_2(\text{a})$	$1.0 \times 10^6$	$2.7 \times 10^0$	$1.0 \times 10^5$	$2.3 \times 10^5$	$2.0 \times 10^5$	$1.8 \times 10^5$	$1.0 \times 10^3$	$1.1 \times 10^2$
$\text{C}_2(\text{X})$	$1.0 \times 10^5$	$9.4 \times 10^{-1}$	$4.0 \times 10^4$	$1.5 \times 10^5$	$6.0 \times 10^4$	$1.3 \times 10^5$	$1.0 \times 10^0$	$1.1 \times 10^1$
$\text{C}_2\text{H}_2$	$4.0 \times 10^{17}$	$1.4 \times 10^{16}$	$2.8 \times 10^{11}$	$1.8 \times 10^{11}$	$3.7 \times 10^{12}$	$1.8 \times 10^{12}$	$3.0 \times 10^{13}$	$1.1 \times 10^{13}$

## ACKNOWLEDGMENTS

The authors wish to thank Mike Ashfold, Neil Fox and Keith Rosser for useful discussions and suggestions. The Bristol-Moscow collaboration is supported by a Royal Society Joint Project Grant, and Y.A.M. acknowledges support from the RF Government for Key Science, Schools grant No. 3322.2010.2.

## REFERENCES

1. P. W. May, *Science* **319**, 1490 (2008).
2. P. W. May, *Philos. Trans. R. Soc. Lond. Ser. A* **358**, 473 (2000).
3. A. Netto and M. Frenklach, *Diamond Relat. Maters.*, **14**, (2005) 1630.
4. P. W. May, N. L. Allan, J. C. Richley, M. N. R. Ashfold, Yu. A. Mankelevich, *J. Phys. Cond. Matter* **21**, 364203 (2009).
5. P. W. May, J. N. Harvey, N. L. Allan, J. C. Richley, Yu. A. Mankelevich, *J. Appl. Phys.*, **108**, 014905 (2010).
6. P. W. May, J. N. Harvey, N. L. Allan, J. C. Richley, Yu. A. Mankelevich, *J. Appl. Phys.*, **108**, 114909 (2010).
7. J.E. Butler, Y.A. Mankelevich, A. Cheesman, J. Ma, M.N.R. Ashfold, *J. Phys.: Cond. Matter* **21**, 364201 (2009).
8. P. W. May, Yu. A. Mankelevich, *J. Phys. Chem. C* **112**, 12432 (2008).
9. A. D. Terekhov, E. N. Frolova, *J. Appl. Mech. Tech. Phys.*, **13**, 582 (1972).
10. M. Eckert, E. Neyts and A. Bogaerts, *Cryst. Eng. Comm.* **11**, 1597 (2009).
11. M. Eckert, E. Neyts and A. Bogaerts, *Cryst. Growth Des.* **10**, 3005 (2010).